The molecular effect of wearing silver-threaded clothing on the human skin

Authors
Alexey V. Melnik[1,7,8,11], Chris Callewaert[2,11], Kathleen Dorrestein[1,11], Rosie Broadhead[9], Jeremiah J. Minich[12], Madeleine Ernst[1,13], Greg Humphrey[2], Gail Ackermann[2], Rob Gathercole[3], Alexander A. Aksenov[1,7,8], Rob Knight[2,4,5,10], Pieter C Dorrestein[1,2,5,6]

1. Collaborative Mass Spectrometry Innovation Center, Skaggs School of Pharmacy and Pharmaceutical Sciences.
2. Department of Pediatrics, University of California San Diego, La Jolla, CA
3. Whitespace Innovation Team, Lululemon, Vancouver, BC, Canada
4. Department of Computer Science and Engineering, University of California, San Diego, La Jolla, CA 92093.
5. Center for Microbiome Innovation, University of California, San Diego, La Jolla, CA 92307.
6. Department of Pharmacology, University of California, San Diego, La Jolla, CA 92037
7. Department of Chemistry, University of Connecticut, Storrs, CT 06269
8. Arome Science Inc, Farmington, CT, 06032
9. Center for Microbial Ecology and Technology, Ghent University, Ghent, BE
10. Department of Bioengineering, University of California San Diego, La Jolla, CA
11. Joint first authors
12. Plant Molecular and Cellular Biology Laboratory, The Salk Institute for Biological Studies, La Jolla, CA
13. Section for Clinical Mass Spectrometry, Danish Center for Neonatal Screening, Department of Congenital Disorders, Statens Serum Institut, Copenhagen, Denmark

Author contributions:
KD and PCD Study and experimental design.
KD experimental organisation and set up.
KD, CC: metabolite and microbial sample collection.
AVM, AA: mass spectrometry data collection.
AVM, AA: mass spectrometry data analysis.
GH 16S rRNA sequencing.
CC, GA: metadata organisation.
CC, JJM: microbial data analysis.
ME: Heatmap of chemical classes.
AVM, AA, CC, KD, PCD, RK, RB: wrote the manuscript.

All authors critically revised the manuscript for important intellectual content.

To whom correspondence should be addressed regarding microbial sequencing rknight@ucsd.edu, for mass spectrometry, sampling, and the project itself pdorrestein@ucsd.edu

Abstract

With growing awareness that what we put in and on our bodies affects our health and wellbeing, little is still known about the impact of textiles on the human skin. Athletic wear often uses silver threading to improve hygiene, but little is known about its effect on the body's largest organ. In this study we investigated the impact of such clothing on the skin's chemistry and microbiome. Samples were collected from different body sites of a dozen volunteers over the course of twelve weeks. The changes induced by the antibacterial clothing were specific for individuals, but more so defined by gender and body site. Unexpectedly, the microbial biomass on skin increased in the majority of the volunteers when wearing silver threaded t-shirts. Although the most abundant taxa remained unaffected, silver caused an increase in diversity and richness of low-abundant bacteria and a decrease in chemical diversity. Both effects were mainly observed for women. The hallmark of the induced changes was an increase in the abundance of various monounsaturated fatty acids (MUFAs), especially in the upper back. Several microbes-to-metabolites associations were uncovered including *Cutibacterium,* detected in the upper back area, that was correlated with the distribution of MUFAs; and *Anaerococcus* spp. found in the underarms, which were associated with a series of different bile acids. Overall these findings point to a notable impact of the silver threaded material on the skin microbiome and chemistry. We observed that relatively subtle changes in the microbiome result in pronounced shifts in molecular composition.

Introduction

In recent years, there has been a fundamental shift in our understanding of the innate chemistry of the body and the role the microbiome plays in shaping it. Individual chemistries, the molecular makeup of our bodies, are influenced by a multitude of genetic and environmental factors. Some are known to have a profound influence (in particular, the diet), while the role of other factors such as the clothing and products we wear on our skin are less explored[1,2,3]. The skin is home to an estimated 10^{12} microorganisms that live and feed on the skin secretions[4]. These billions of microorganisms, including bacteria, fungi, protists and viruses, form the so-called skin microbiome [5,6]. The role of the microbiome, in particular, has been uncovered, time and time again, as a key factor in a number of pathologies[7,8]. A community of microorganisms creates an environment that enables the skin to be less susceptible to diseases and pathogenic invasion, and therefore microbial diversity and a healthy immune system are inherently linked[7, 3,6].

There has been an appreciation for the role of skin microbes, and their interaction with clothing for aspects such as body malodour[2]. Yet, the ways and effects of altering skin microbiota with clothing and the corresponding effects on health and well-being are not known, but are a growing subject of research[9]. In large part due to the activity of the microbiome, the skin contains various low molecular weight compounds (metabolites). Some of these compounds are either by-products of endogenous or microbial metabolism and others are implemented as part of the skin's physiological role[10]. The metabolome along with the microbiome represents the body's first barrier to external and environmental substances. Through these metabolic pathways the skin transfers topical signals to determine the body’s physiological activities and regulate homeostasis. Thereby, these processes are adapted to varying external factors, such as cosmetic, clothing or other environmental influences. Many of the same enzymes which operate in the liver also inhabit the skin, as such the skin is an important metabolically active organ[11,12]. The skin surface can be sampled to detect and quantify skin metabolites related to diseases, through secreted sweat. Through techniques such as chromatography-mass spectrometry (MS) and other methods, broad spectrum skin metabolite specimens can be characterised[10]. These biomarkers are an important tool for the diagnosis and treatment of skin diseases, and how environmental factors may be of influence[13,14].

Consequently, skin metabolome and microbiome analysis can be a useful indicator in the investigation of the effects of various external stimuli. One of these external stimuli include the incorporation of antibacterial agents into a fabric, for example, the use of metallic and synthetic antimicrobial biocides for odour control in textiles. The increase of antimicrobial agents in our everyday products including our clothing has made it difficult to re-establish or maintain the beneficial bacteria that the

body would regularly be exposed to in a more natural environment[15]. One of the most common antimicrobial additives is the incorporation of silver ions or nanoparticles. Silver has broad-spectrum antibacterial properties against Gram-positive and -negative bacteria. In particular, X-static textiles, a silver coated yarn threaded fabric, are currently used in sports clothing for odour control, hygiene, and social comfort, which can thereby enhance product performance. Overall there has been an increased demand in the antibacterial effects of metal ions, such as silver in the textiles industry[16,17–19].

However, the influence of such antimicrobial clothing on the skin microbiome, and, especially, metabolome is largely unknown. By learning about the resulting perturbations of microbial communities or body chemistries it may be possible to then manipulate the effects, including those on health by designing the composition of clothing. In this study, we have analysed skin metabolome and microbiome throughout several weeks of wearing the silver coated yarn threaded Tt-shirt to document the changes caused by the antibacterial effect of silver. Several studies have analysed the microorganisms associated with body odour and the bacteria present on malodorous textile[20,21]. This is the first study to explore the influence of the antibacterial properties of silver threaded textiles on the skin microbiome, metabolome and its subsequent influence on the textile microbiome and metabolome. The skin's unique microenvironments were also observed through multiple sample locations across the body. This is an important area of research to determine how antimicrobial textiles affect both the skin microbiome and chemistry, and how these two environments are interlinked.

Results

Metabolome results

This study aimed to investigate the impact of antibacterial silver-threaded clothing material on the human skin metabolome and microbiome in a controlled manner. The experiment took place over the course of 12 weeks for the total of twelve volunteers: six males and six females (**Supplementary Figure 1**). Four body sites: chest, upper back, lower back and armpits were chosen for sampling because of the most immediate contact with the closing material **(Supplementary Figure 1b)**. As described in the Materials and Methods, the experiment longitudinally spanned a total of four phases: initial wash-out, silver-threaded t-shirts, regular t-shirt and silver-threaded t-shirts again **(Supplementary Figure 1a)**. During the study course, volunteers were prompted to use only the provided skin products to minimise variability. The full sample set included samples from skin, clothes and the skin products that volunteers have been using.

We have then conducted untargeted LC-MS/MS analysis as described in Materials and Methods. The resultant data were subjected to molecular networking on GNPS[22]. The molecular networking represents all unique compounds as network nodes and those with similar MS/MS spectra are connected by edges. Since structurally similar compounds tend to also have similar fragmentation patterns, molecular networking enables visualising chemical relationships within the dataset. The **Figure 1a and 1b** shows molecular networks of all compounds that were detected in this study. Colouring the nodes according to, for example, different body parts **(Figure 1a)** or Tt-shirt phase **(Figure 1b)** gives visualisations of associated molecular distributions.

Our results indicate that silver threaded fabric indeed induces changes of skin chemistry that are detectable with an untargeted approach used in this study. Several observations could be made: one interesting finding is a notable decrease in the chemical diversity for samples of all except for one volunteer during the silver shirt usage phase **(Supplementary Figure 2c)**. When combined, the differences in Shannon diversity of metabolites was significant and were more pronounced for females ($p=1.9e-05$) than for males ($p=0.0027$) **(Supplementary Figure 2a, 10)**. A persistent challenge in skin studies is the overwhelming signal contribution from skin products, especially deodorants[23]. Since the application of deodorants is mostly limited to armpits, we have further considered the body parts separately. The highest impact on the chemical diversity was observed for lower and upper back ($p=1.1e-04$ and 0.0038, respectively), while no significant effect was found on chest ($p=0.26$) and armpit ($p=0.42$) **(Supplementary Figure 2b, 10)**.

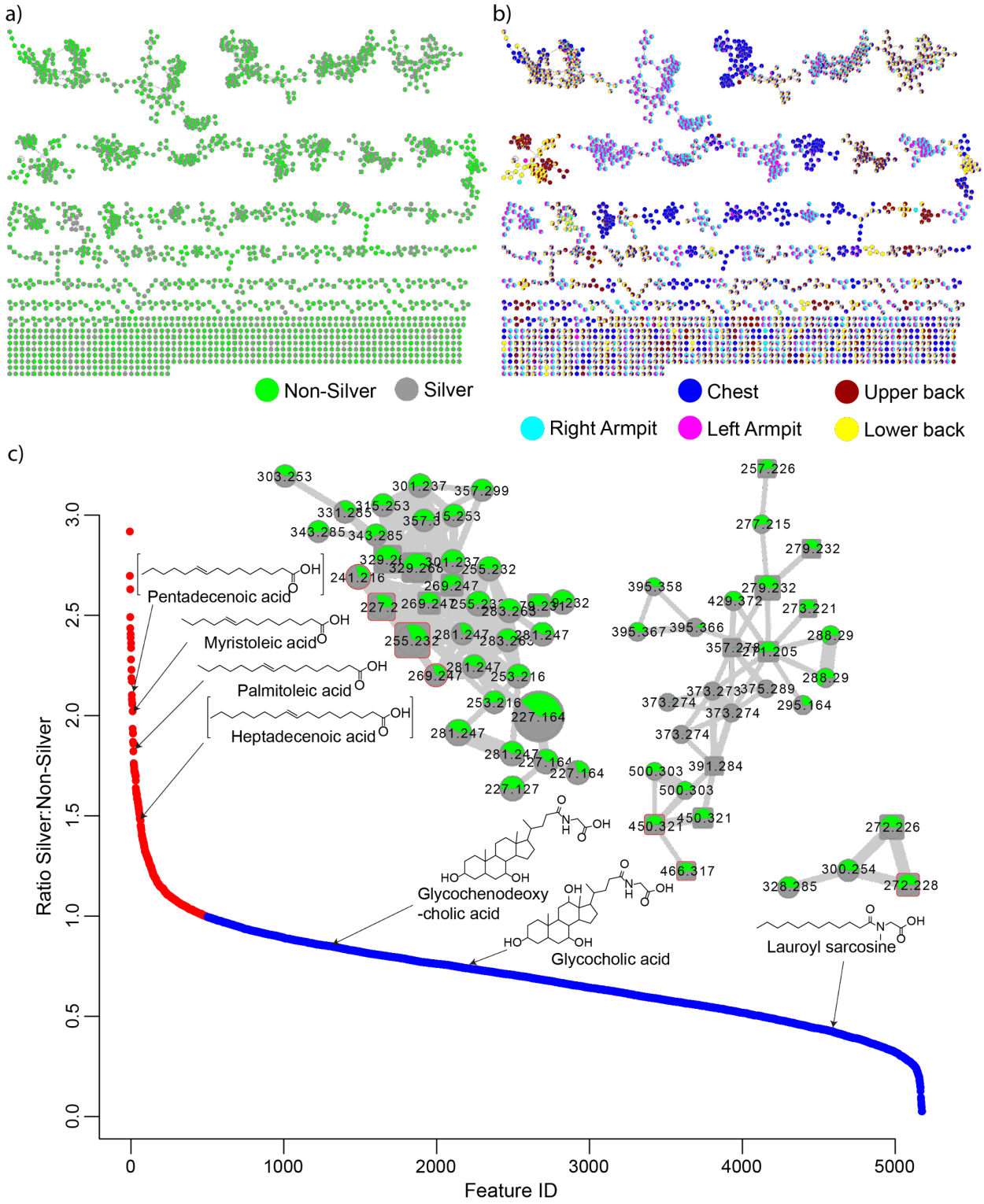

Figure 1. Molecular networks for exploration of metabolome changes induced by silver fabric. Global molecular networks of metabolomics data colour-coded by a) Tt-shirt phase and b) body part. c) The plot showing the ratio of abundances of metabolites during the silver versus non-silver phases on upper and lower back. Ratios higher and lower than one (i.e. molecules that increased and decreased in abundance) are highlighted in red and blue, respectively. Examples of some of the annotated molecules

with the corresponding clusters from the molecular network that contain them are shown: monounsaturated fatty acids; bile acids and a surfactant. Clusters are coloured the same way as in panel a). Consistent ratios of MUFAs' abundances across the cluster are suggestive of the same chemical forces responsible for the changes in their differences in silver vs. non-silver samples. The depicted compounds are highlighted by square nodes.

We have visualised the metabolome on principal coordinates (PCoA) plot with Canberra dissimilarity metric using the Emperor software[24](**Supplemental Figure 3**). The main factor driving differences is the sampled body part, which appears to be even more significant than the sampled subject (**Supplementary Figure 3a**). Interestingly, armpit samples spanned across full PC1 space and were separated into two distinct clusters along PC2 and PC3 axis interpreted as two armpits (**Supplementary Figure 3b and 3c**). The textile and the skin chemistry differs in the underarms as compared to the textile worn next to it (**Supplementary Figure 3c**). Notably, a clear separation of left and right axilla was observed for 8 out of 12 volunteers. (**Supplementary Figure 3c**) This discordance was also confirmed by the diversity analysis - the higher chemical diversity in the left armpits of these eight volunteers was observed for both males and females (p=0.023) (**Supplemental Figure 10d**). It is known that there exists a fraction of the population that has distinct microbiomes in their left and right axilla[25]. A number of compounds that may be linked to bacterial origin - acylcarnitines, phospholipids and bile acids have been found to have different abundances in two armpits **(Supplementary Figure 4)**. Using random forest analysis, we have confirmed that antiperspirant constituents are more abundant in the left armpits, possibly due to more vigorous application by dextrous vs. sinistrous volunteers. This finding was corroborated by matched clothing armpit samples (**Supplemental Figure 3a**). Based on our data, we hypothesised that the contribution to the discrepancy in the chemical diversity is both due to the chemical constituents of deodorant, but also differences in microbial ecosystems. For both types of participants, with concordant and discordant chemical signatures in axillae, the silver threaded clothing did not induce differences in axillae chemistries that could be observed with the Canberra distance metric.

When considering body parts separately, the effects of silver could be more clearly observed. **Figure 2a** and **2b** shows PCoA plots for the upper and lower back samples where these differences were found to be especially pronounced; **Figure 2c** shows the volcano plot for these samples. After examining the most significant discriminating features, we have discovered that they predominantly belong to a single network cluster shown on **Figure 1c**, indicating their structural similarity. The annotations for these compounds were then established as a variety of monounsaturated fatty acids (MUFAs). The key drivers of the differences include Palmitoleic acid, Myristoleic acid and Pentadecenoic acid. All of these compounds

change in unison in response to wearing silver-threaded t-shirts and were detected in similar abundances (**Figure 2d**). The relative abundance of pentadecenoic acid (C15 MUFA) increased during the silver Tt-shirt phase, while its abundance decreased during non-silver Tt-shirt phase (**Figure 3d**). The presence of odd-carbon short chain fatty acids (OCS-FAs) among these discriminating compounds strongly suggests their microbial origin. From our data, it appears that silver fabric alters the bacterial populations on skin in a way that results in accumulation of MUFAs.

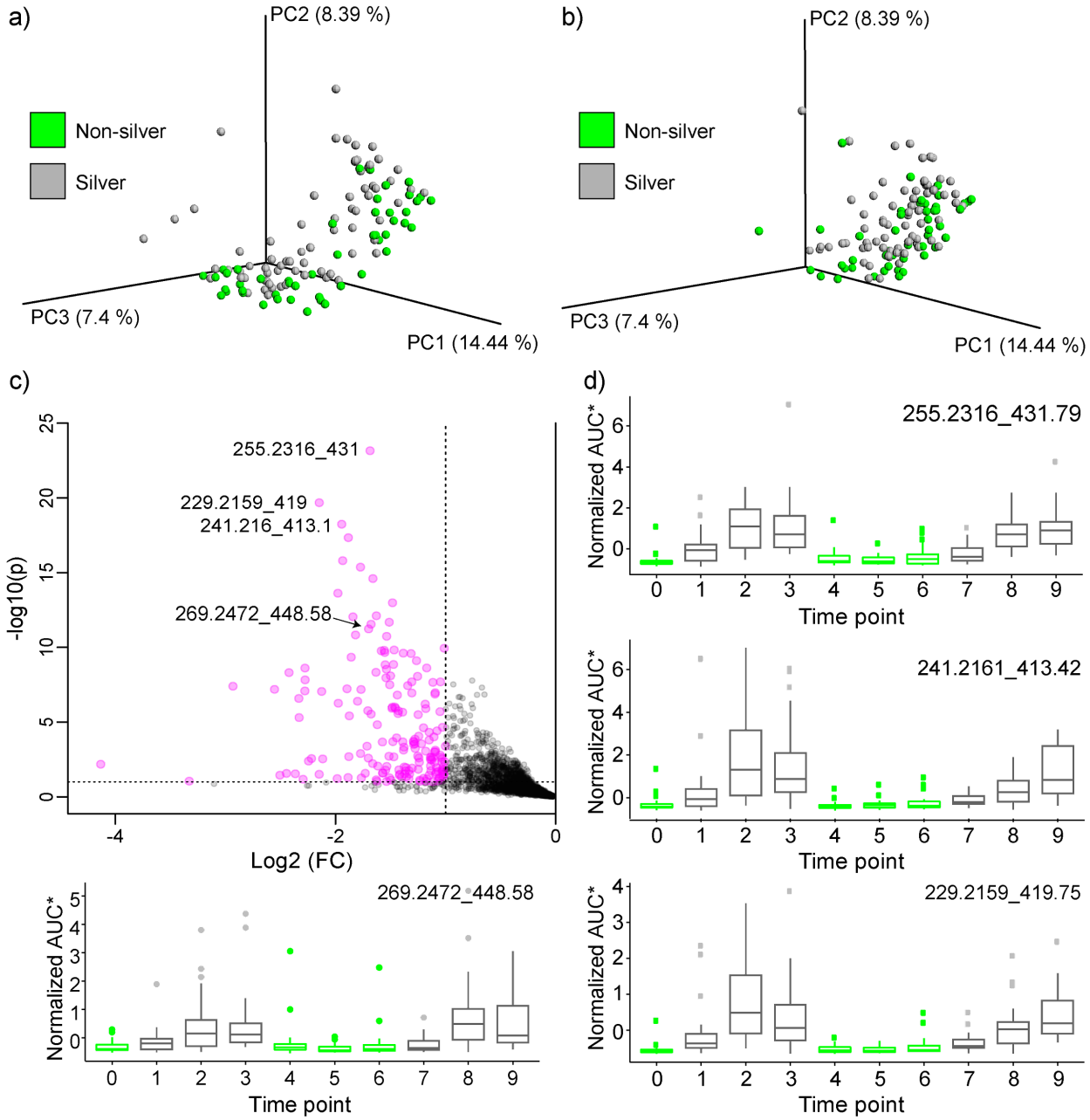

Figure 2. Monounsaturated fatty acids are the key compounds on skin affected by silver. a) and b): PCoA plots (Canberra distance) of metabolomics data for upper and lower back respectively, showing the

differences of molecular profiles induced by silver. c) Volcano plot for upper and lower back samples showing most significant metabolites enriched by silver. The features for some MUFAs are labelled (parent m/z_retention time). d) Box plots plotted over a time period of sampling for several MUFAs in combined upper and lower back samples.

Microbiome results

The paired microbiome analysis has yielded several observations that help to understand the metabolomics findings. Counterintuitively, the skin and textiles bacterial communities had a higher bacterial biomass when silver Tt-shirts were worn, compared to non-silver Tt-shirts (p=0.0011, Mann Whitney U-test) (**Figure 3a, Supplementary Figure 5d**). The results were different for every individual, with 10 of the 12 volunteers showing more skin bacteria during the silver phase, one volunteer no change and one lower (**Supplementary Figure 5b**). This is unexpected, as considering the antibacterial properties of silver ions has been widely reported[26]. It has been shown that bacteria are readily transferred onto the shirt material in the armpit region[2]. Silver textiles can manipulate the microbiome and metabolome of the skin, but, importantly, do not reduce microbial biomass. Additionally, it is known that resident microbial strains which cause body odour are due to the presence of certain microbes rather than biomass[20].

Microbe-metabolite co-occurrences were explored using microbe-metabolite vector co-occurrence analysis (mmvec) **(Figure 3)**, a neural network-based approach that aims to predict metabolite abundances given the presence of a single microbe, and vice versa[27]. We detected a range of primary bile acids in the underarms of participants, including glycocholic acid and glycochenodeoxycholic acid. Such bile acids were not detected in other skin body sites. Bile acids were detected in the underarms of all participants, although high inter-individual differences were seen in bile acid concentration. The mmvec plot shows co-occurrence of *Anaerococcus* spp. and these bile acids (**Figure 3e**). All identified bile acids were significantly correlated with relative abundance of *Anaerococcus* spp. (p=4.903e-05, Spearman correlation) (**Figure 3c**, **Supplementary Figure 9a**) and were more abundant in armpits compared to back and chest (**Supplementary Figure 9d**). *Anaerococcus* spp. were similarly more abundant on armpit skin as compared to chest skin (p=0.00027) and back (**Supplementary Figure 9c**). Interestingly, the bile acids were generally decreased in the silver phase (**Supplementary Figure 9b**).

As noted in the previous section, during the silver Tt-shirt phase, we have identified enrichment of a series of monounsaturated fatty acids (MUFAs), particularly on skin of chest, upper back and lower back, as a hallmark feature (**Figure 2**), and presence of odd-number carbon acids indicates that at least some of these compounds can only originate from food or bacterial metabolism. From mmvec analysis, *Corynebacterium* spp. Were found to be one of the species that tend to co-occur with MUFAs (**Figure 3f**). Other microbial species also appear to play a role in the increase of

MUFAs during the silver phase. For example, we found a strong correlation of MUFA abundances (myristoleic acid) with the relative abundance of *Cutibacterium* spp. ($p<2.2e-16$, Spearman test) (**Supplementary Figure 6a,f**), suggesting these bacteria may also be involved in their biotransformation. Random Forest regression analysis showed the highest contribution of *Cutibacterium*, as compared to all other bacterial taxa (**Supplementary Figure 6e**). We found that *Cutibacterium* spp. were enriched with silver t-shirts on both t-shirts ($p=0.04$, Mann Whitney U-test) (**Figure 3b** and **Supplementary Figure 6c)** and on the skin itself (LDA score increase = 2.7) (**Supplementary Figure 6c**). We also found a correlation between C14 MUFA ($p=0.0124$, Spearman test) and C17 MUFA ($p=2e-04$, Spearman test) and the bacterial biomass on the skin of the back, suggesting that bacteria and their biomass are involved in the bioconversion of MUFAs.

The impact was the largest where the contact between silver clothes and skin was the highest: upper back and chest skin. During the silver phase, the skin of the torso (chest and back) became enriched in *Lactobacillus*, *Anaerococcus*, *Gemellaceae*, *Cutibacterium*, and *Lactococcus* ($p<0.05$, Mann Whitney U-test). The silver shirts themselves were enriched in *Cutibacterium* spp. (**Figure 3b**), amongst some other taxa. Anecdotally, volunteer 11 mentioned incident upper back acne when the silver shirts were worn, which might suggest the intermittent increases of relative abundance of *Cutibacterium* spp. on the upper back.

When looking at the log abundance ratios, we notice particular bacterial genera that enrich on skin when wearing silver threaded clothing, as compared to non-silver clothing. Bacterial genera that were consistently more abundant on chest, upper back, lower back when silver clothing are worn are *Bacteroides, Acinetobacter, Peptoniphilus, Akkermansia, Facklamia, Haemophilus, Helcococcus, Rothia, Lactococcus, Erwinia* spp. (Songbird/Qurro results not shown). These small changes in microbial diversity have led to much more significant changes in the skin metabolome, discussed above.

Our results indicate that the skin microbiome is strongly determined by individuality, body site and gender, as reported earlier[28,29]. *Staphylococcus* and *Corynebacterium* were the main bacterial groups in armpit, chest, upper and lower back skin (**Supplementary Figure 7)**. Females had a higher relative abundance of *Staphylococcus* while males had a higher relative abundance of *Corynebacterium*, as documented before[25]. These bacterial groups were not significantly impacted by the silver-threaded textiles and the proportions of the most abundant skin taxa did not change (**Supplementary Figure 8c**). The impact of silver-threaded shirts on the bacterial composition was subtle but noticeable. Silver increased the female skin microbial Shannon diversity significantly ($p=0.036$, Mann Whitney U-test) (**Supplementary Figure 8c**), and was less so affected on chest and upper back ($p=0.05$, Mann Whitney U-test). This diversity difference was not seen on male skin

(p=0.99, Mann Whitney U-test) and is likely outweighed by the more abundant *Corynebacterium* (and *Staphylococcus*) spp. present on male skin (**Supplementary Figure 7a**). Notably, this increase in microbial diversity also corresponds to a decrease in the chemical diversity.

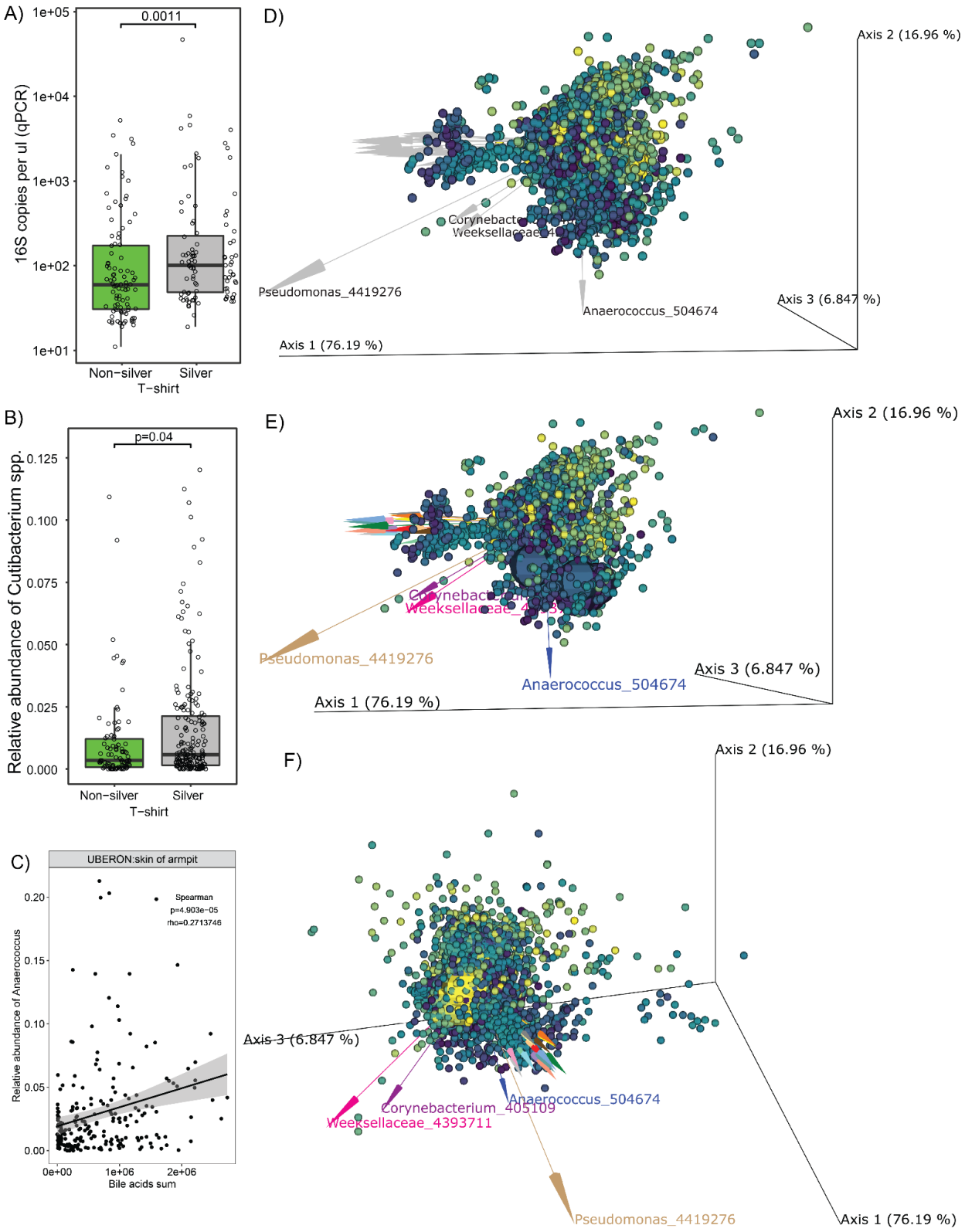

Figure 3. Microbiome metabolome co-occurrence determined by mmvec. a) qPCR and b) bacterial Shannon diversity results of all samples combined and stratified by the Tt-shirt phase, respectively. c)

Cutibacterium spp. distribution by the t-shirt phase d) mmvec biplot showing metabolome, where each sphere is metabolite feature colour-coded based on the enrichment in the silver phase, and microbiome, where each arrow represents a microbe. A proximity of both metabolites and microbes is indicative of their co-occurrence. f) MUFAs tend to co-occur with *Corynebacterium* spp. MUFAs were all enriched in the silver phase (light large spheres). e) Bile acids co-occur with *Anaerococcus* spp. Bile acids were generally decreased in the silver phase (dark large spheres).

Discussion

Silver is the most commonly used antimicrobial agent for textile application, and silver nanoparticles (AgNP) are the most used nanoparticles in consumer products[30]. However, there has been limited research on the physiological responses to such textiles on the skin microbiome and metabolome. In this study, we have found that the material used in clothing can cause changes in the chemistry and microbial community of the skin surface. The impact of clothing on skin chemistry and microbiome is highly individualised and differs for genders and body sites[28,29]. This also corresponds with findings from a study on the Tt-shirt microbiome which found the textile to be highly individual in microbial composition, diversity and biomass[29]. Although in this study, the abundant genera remained unaffected, low-abundant taxa were perturbed and the use of antibacterial Tt-shirts also resulted in higher bacterial biomass on skin. Silver textiles can manipulate the microbiome and metabolome of the skin, but do not reduce microbial biomass.

Silver-coated yarn threaded Tt-shirts had a small but significant impact on the skin microbiome (mainly for females), leading to a higher richness and diversity including higher abundance of some odour-causing species, such as *Anaerococcus*. During the silver phase in male participants, a higher bacterial biomass was found with *Staphylococcus and Corynebacterium* being the most dominant (**Supplementary Figure 5d and 7**). The altered skin microbiome corresponded with a large impact on the skin metabolome.The microbiome and metabolome data suggest that silver textiles alter the bacterial populations on the skin in a way that, most notably, results in the accumulation of monounsaturated fatty acids (MUFAs). These MUFAs were the key compounds on skin affected by the silver textiles (**Figure 2**). All of these compounds changed in unison with the silver phase and were detected in similar abundances (**Figure 2d**). The presence of odd-carbon short-chain fatty acids (OCS-FAs) among these discriminating compounds strongly suggests a microbial origin. Bacteria can produce odd-chain fatty acids related to the production of propionic acid[31,32,33]. A multi-omics analysis suggested a link between the abundance of MUFAs e.g. myristoleic acid and certain microbes, such as *Corynebacterium* and *Cutibacterium* spp. (**Figure 3f and Supplementary Figure 6e**). We hypothesise that the silver-threaded shirts led to a higher sebum production on the skin, which led to higher bacterial biomass and certain species enriched during the silver phase. (**Supplementary Figure**

6b,c,d). Interestingly, this increase in microbial diversity also corresponds to a decrease in the chemical diversity **(Supplementary Figure 7a)**. Yet, the impact of skin cosmetics and antimicrobial ingredients in other studies have led to both an increase in chemical diversity and an increase in microbial diversity[23].

Monounsaturated fatty acids are the major fatty acids that are present in human sebum[34,35]. Corynebacteria are lipophilic bacteria that rely primarily on fatty acids as a food source[36,37,27]. A co-occurrence between MUFAs and Corynebacteria could be due to the ability of the latter to produce FadD enzymes, which is the first step to break down fatty acids in the beta-oxidation pathway[38]. In another example, *Cutibacterium acnes,* Gram-positive skin commensal, has been identified to be a contributing factor to acne on strain level[39]. These species also have the enzymatic capacity to manipulate the MUFAs on the skin[40]. *Cutibacterium* spp. were enriched on the skin of the torso, which corresponded with an increase in the production of medium-chain fatty acids, including odd-carbon ones (**Supplementary Figure 6b**). The silver textile shirts themselves were similarly enriched in *Cutibacterium* spp. **(Supplementary Figure 8f)** and contained fewer staphylococci. Further exploration of microbial involvement into the bioconversion of sebum into MUFAs is warranted. The results further showed a separation of textiles and skin metabolomes and that clothes differ in this respect from the skin sites **(supplementary Figure 3)**. Other studies have shown the composition differences in axillary and textile microbiome, and similarly we saw that the skin and textile metabolome are behaving independent of each other[2].

This study also identified a range of different primary bile acids, which were solely found in the armpits of participants. The mmvec analysis established a clustering of the bile acids in both the silver and non-silver phase. Bile acids may help in solubilizing underarm lipids, which can help reduce friction in the underarm. In our study, these bile acids were associated and correlated with *Anaerococcus* species (**Figure 3e**). *Anaerococcus* is a low abundant species in the underarm and associated with higher malodour scores[21]. Bile acids are host-produced by the apocrine sweat glands[41] and were detected only in the underarms[23]. Bile acids have an important role in lipid metabolism in the gut to manage the microbial community, therefore, it has a therapeutic role against pathogens[42,43,44]. However, the function of bile acids on the skin remains largely unknown[42]. The results of a study found certain probiotic bacteria including *Lactobacillus*, *Bifidobacterium* and *Bacillus* to be resistant to bile acids, thus reducing bile acids relative antimicrobial activity[45,46]. This suggests the selective capabilities of bile acids on certain strains of bacteria. In this paper the silver textile has caused slight distortion in the microbial community, which has led to these larger changes in metabolism on the skin.

Conclusion

In this study, we investigated the impact of clothes with antimicrobial properties on the skin by studying induced changes of microbiome and metabolome. The main changes to the skin microbiome and metabolome include an increase of bacterial biomass and an increase of monounsaturated fatty acids in the silver phase. The observation of bile acids on the skin was found in the silver and non-silver phase. Bile acids have an important role in lipid metabolism in the gut but function on the skin remains unknown. This study indicates that the microbiome and metabolome are interlinked, and the textiles did indeed cause changes on the skin microbiome which drove significant chemical changes on the skin due to silver antimicrobials. Textile and its active ingredients do have an impact on human skin biology and chemistry and may provide a direct way to manipulate skin chemistry for health and wellbeing. However, more extensive research is needed on more volunteers into the strain significance of the microbiome changes, and the exact origin of the chemical changes on the skin.

Materials and methods

Study Design

Healthy volunteers were enrolled in this study with one visit every week for 11 weeks. Personal care products and laundry detergent were provided to all volunteers used in the study. Shower during the 11 weeks study was allowed only with the shampoo, soap and deodorant that were provided. During the washout period, the first two weeks, participants asked to wear the non x-static shirt. During the first 3 weeks, post washout period, participants asked to wear the x-static shirt. Following by wearing the non x-static shirt on week 4 to week 6, and finish with X-static yarn threaded t-shirt again. X-Static yarn is treated with silver to inhibit the growth of bacteria on fabrics, eliminating human-based odour (https://noblebiomaterials.com/x-static/). The amount of x-static yarn was 5% for the female shirt and 4% for the male shirt. Non x-static shirts are not treated with silver. Participants were asked to take no shower 24 hours before sample collection.

Sample collection

A sterile swab, either with alcohol solution or saline solution, was used to collect samples from small skin areas (2 x 2 inch) by swabbing the skin surface for approximately 10 seconds. 2 samples from 5 body sites were collected for a total of 10 samples per volunteer per week. The samples were collected from the right armpit, left armpit, upper back, lower back, and chest. After collection, the swabs were put in a 96 well plate (one for metabolite and one for sequencing), containing the appropriate extraction buffer.

DNA extraction and sequencing

16S rRNA gene amplicon sequencing was performed following the Earth Microbiome Project protocols[47], as described before[42]. Briefly, DNA was extracted using MoBio PowerMag Soil DNA Isolation Kit and the V4 region of the 16S rRNA gene was amplified using barcoded primers[48]. PCR was performed in triplicate for each sample, and V4 paired-end sequencing[48] was performed using Illumina HiSeq (La Jolla, CA, USA). Raw sequence reads were demultiplexed and quality controlled using the defaults, as provided by QIIME 1.9.1[49]. The primary OTU table was generated using Qiita (https://qiita.ucsd.edu/), using UCLUST[50] closed-reference OTU picking method against GreenGenes 13.5 database[51]. Sequences can be found in EBI under accession number EBI: ERP138010 or in Qiita (qiita.ucsd.edu) under Study ID 11272.

qPCR

We analysed the absolute quantity of bacteria on a subset of the samples, using qPCR. A total of 192 samples were processed for qPCR 16S rRNA gene quantitation which included 168 primary samples and 24 DNA extraction blanks as reference. Specifically, 1 ul of neat gDNA from each of the 12 volunteers at week 8 (non-silver phase) and week 11 (silver t-shirt phase) along with each sample site including right armpit, left armpit, chest, lower back, upper back, left armpit clothing, and right armpit clothing was amplified in a 10 ul PCR reaction with DyNAmo HS SYBR green mastermix (ThermoFisher Cat # F410L) in triplicate for qPCR analysis on the Roche LightCycler 480 using the same amplification conditions and primers (16S primers 515f and 806rb) as described for the microbiome analysis. An isolate of Vibrio fischeri ES114 with known genome size and gDNA concentration, determined with a Qubit (ThermoFisher) was 10 fold serially diluted six times (135000 - 1.35 genome copies) and included used as a positive control. The qPCR amplification efficiency was 95.68% and 93.34% for the two qPCR runs. The conservative level of detection was 135 copies for each run with the R2 being 0.99749 and 0.99724 for the two runs. Reported values are in 16S rRNA gene copies per ul. Since each gDNA extraction was 100 ul, one could multiply by 100 to indicate total 16S RNA gene copies per DNA extraction, but we have chosen to leave this in the original form of copies per ul.

Metabolites extraction and UPLC-Q-TOF MS/MS analysis

Skin swabs were extracted and analysed using a previously validated workflow described in[52]. All samples were extracted in 200 µl of 50:50 ethanol/water solution for 2 h on ice then overnight at − 20 °C. Swab sample extractions were dried down in a centrifugal evaporator then resuspended by vortexing and sonication in a 100 µl 50:50 ethanol/water solution containing two internal standards (ISTDs). The ethanol/water

extracts were then analysed using a UPLC-MS/MS method described in[42]. ThermoScientific Dionex 3000 UPLC for liquid chromatography and a Maxis Impact II mass spectrometer(Bruker Daltonics), controlled by the software packages (Bruker Daltonics) and equipped with ESI source were used. UPLC conditions of analysis are 1.7 µm C18 (50 × 2.1 mm) UHPLC Column (Phenomenex), column temperature 40 °C, flow rate 0.5 ml/min, mobile phase A 99.9 water /0.1 formic acid (v/v), mobile phase B 99.9 acetonitrile/0.1 formic acid (v/v). A linear gradient was used for the chromatographic separation: 0–2 min 0–20% B, 2–8 min 20–99% B, 8–9 min 99–99% B, 9–10 min 0% B. Full-scan MS spectra (m/z 80–2000) were acquired in a data-dependant positive ion mode. Instrument parameters were set as follows: nebulizer gas (nitrogen) pressure 2 Bar, capillary voltage 4500 V, ion source temperature 180 °C, dry gas flow 9 l/min, and spectra rate acquisition 10 spectra/s. MS/MS fragmentation of 10 most intense selected ions per spectrum was performed using ramped collision induced dissociation energy, ranged from 10 to 50 eV to get diverse fragmentation patterns. MS/MS active exclusion was set after 4 spectra and released after 30 s. Mass spectrometry data for this study can be found here: MSV000081379.

LC-MS data processing

LC-MS raw data files were converted to mzXML format using msConvert(ProteoWizard). MS1 features were selected for all LC-MS datasets collected using the open-source software MZmine2[53] and tabulated in the supplementary table S1 for parameters. Subsequent blank filtering, total ion current, and internal standard normalisation were performed for representation of relative abundance of molecular features and for principal coordinate analysis (PCoA).

Microbiome data analysis

All sequence data were quality filtered to discard sequences with a quality score of <20. OTUs and assigned taxonomy using the Greengenes (v13_8) reference database. Samples were rarefied to 2580 sequences per sample, and alpha diversity for each sample and distances between samples were calculated using QIIME v1.9.1[49]. Pairwise differences in alpha diversity were tested using the non-parametric Wilcoxon tests. Taxonomy abundance log-fold differentials were calculated through QIIME2 using the Songbird plug-in[54] with visualisation using Qurro[54,55].

Random forest analysis[56]

A random forest classification model was used to identify microbes and metabolites that separated the textile phases. This model was run using the randomForest package in R

with 5,000 trees and 59 variables tried at each split and with stratification due to differential sample numbers in each disease class.

LEfSe[57]

We used the linear discriminant analysis (LDA) effect size (LEfSe) method (http://huttenhower.sph.harvard.edu/lefse/) for microbe and metabolite biomarker discovery, which performs a combined assessment of statistical significance and biological relevance. The tool utilises non-parametric Kruskal-Wallis test to investigate group differences, using a sample-wise normalised matrix of relative abundances and determines the effect size of a given taxon using LDA. We performed this analysis using the default settings (alpha = 0.05, effect-size threshold of 2).

Mmvec

Microbe-metabolite cooccurrence probabilities were calculated using mmvec, a neural network approach trained to predict metabolite abundances given the presence of a single microbe[27]. This model was trained using three principal axes with a batch size of 10,000 and 10,000 epochs. Mmvec performs cross-validation by evaluating how well the metabolites can be predicted solely from the microbe abundances in the samples.

qPCR statistics

Sample sites were compared using a non-parametric Kruskal Wallis test with multiple comparisons applying the Benjamini-Hochberg FDR. To compare the specific body sites from the effects of silver t-shirt wear, a one-tailed Wilcoxon matched-pairs signed rank test was used to compare statistical differences between use of silver t-shirt across body sites (paired data - per individual).

Supplementary Figures

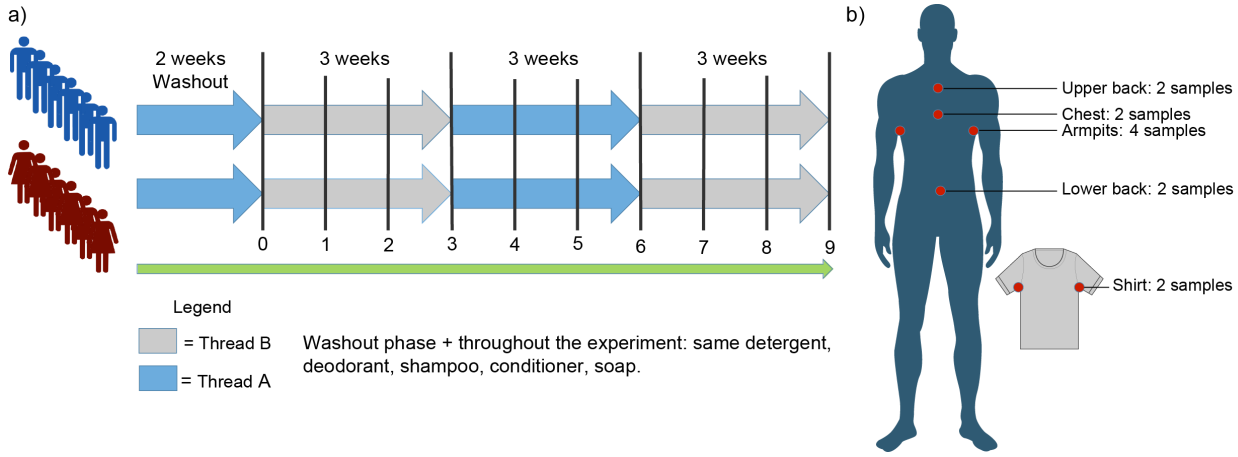

Supplementary Figure 1

Experimental design. a) During 12 weeks, six males and six females were recruited, the first two weeks served as a wash-out period for their own personal care products, and volunteers were asked to use the personal care products provided by the researchers. The following three weeks volunteers wore silver-threaded t-shirts, after which they wore the same but non-silver threaded t-shirts for three weeks, after which they wore the silver-threaded t-shirts again. The skin of the volunteers was sampled every week. The t-shirts were sampled once in the last six weeks. b) All volunteers were sampled on their torso, where the t-shirt touches the skin. Samples were taken from the armpit (left and right), chest, upper back and lower back. Volunteers were asked to follow specific instructions for the use of skin care products.

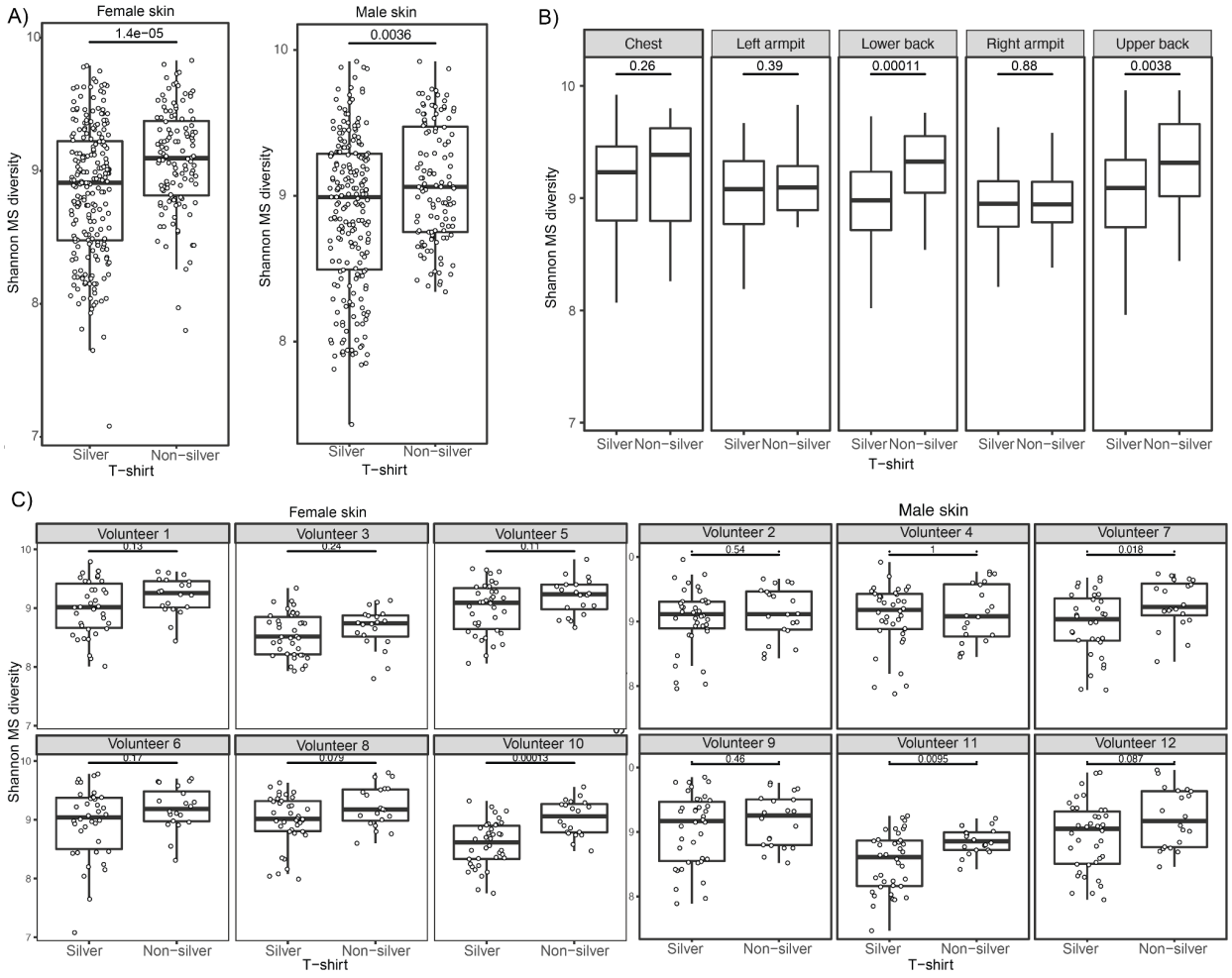

Supplementary Figure 2

Mass spectrometry chemical diversity separated by silver vs non-silver t-shirt phase. Shannon diversity calculated for and combined by: a) gender b) body part sampled c) volunteer assigned number.

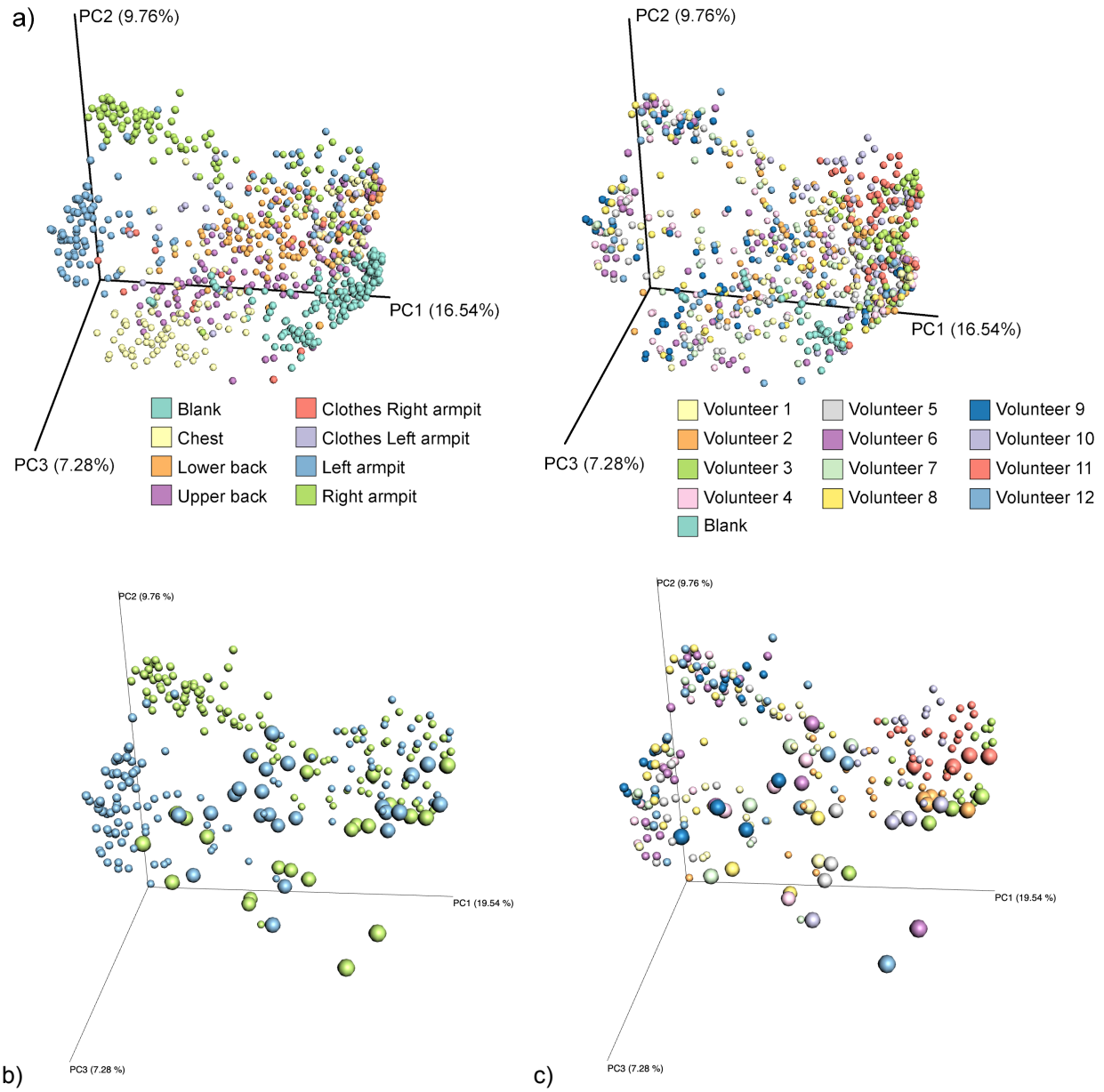

Supplementary Figure 3

General characterization of metabolomics data. a) Principal coordinate analysis coloured by the two most prevalent separation based on body site (left) and volunteer sampled (right). b) Principal coordinate analysis highlighting only armpit samples and coloured based on which armpit side of the body was sampled the same as in a) on the left. Enlarged spheres show samples from t-shirt material adjacent to armpits. c) Similar plot and coloured the same as in a) on the right. Several volunteers' armpit samples express distinct clustering between actual armpits and clothing adjacent to that armpit.

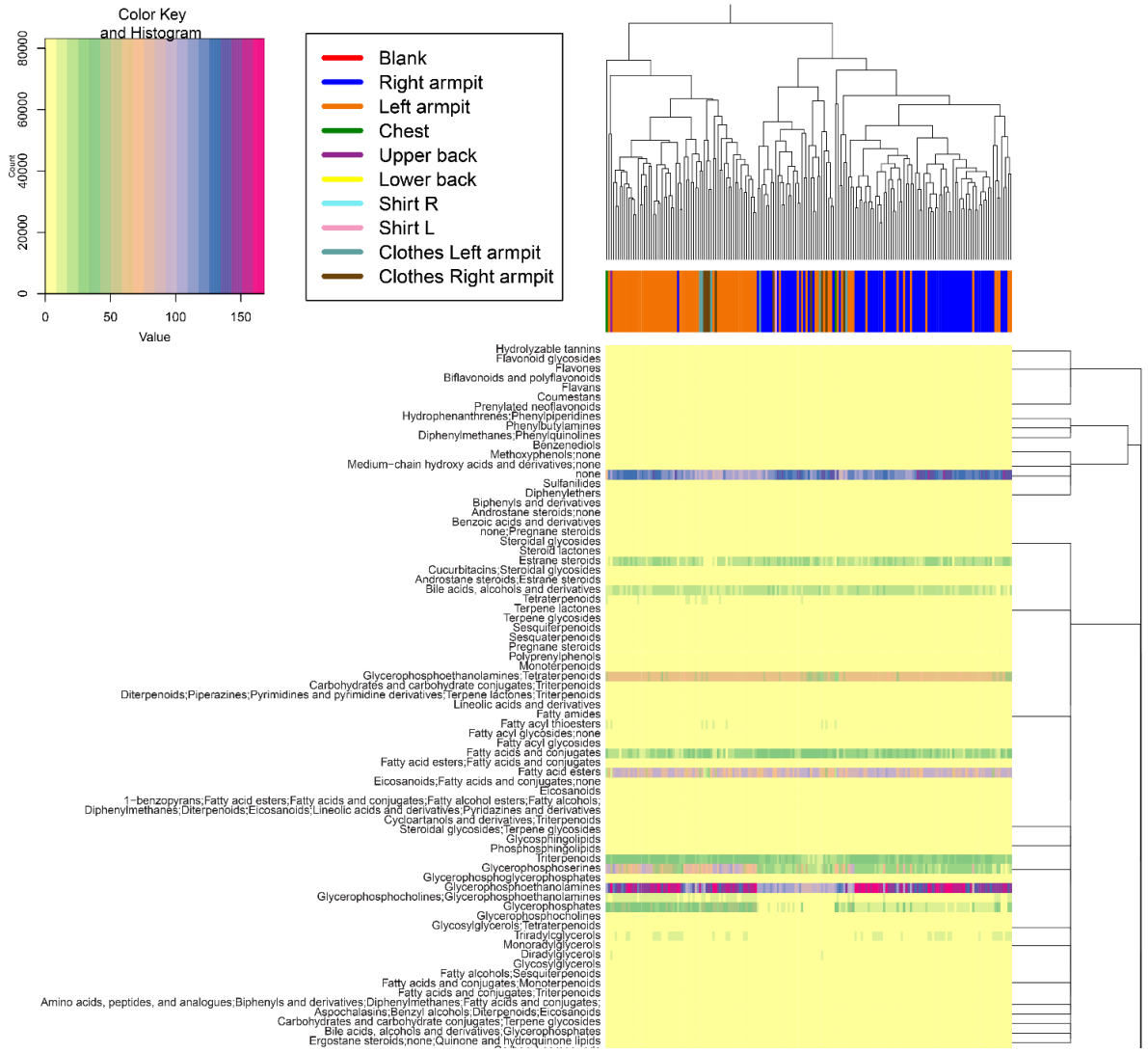

Supplementary Figure 4

Heatmap of metabolites from armpits that have different distributions within left and right armpit samples of all volunteers combined. Chemical classes are putative estimates retrieved through the MolNetEnhancer[58] workflow and based on similarities in MS2 fragmentation patterns.

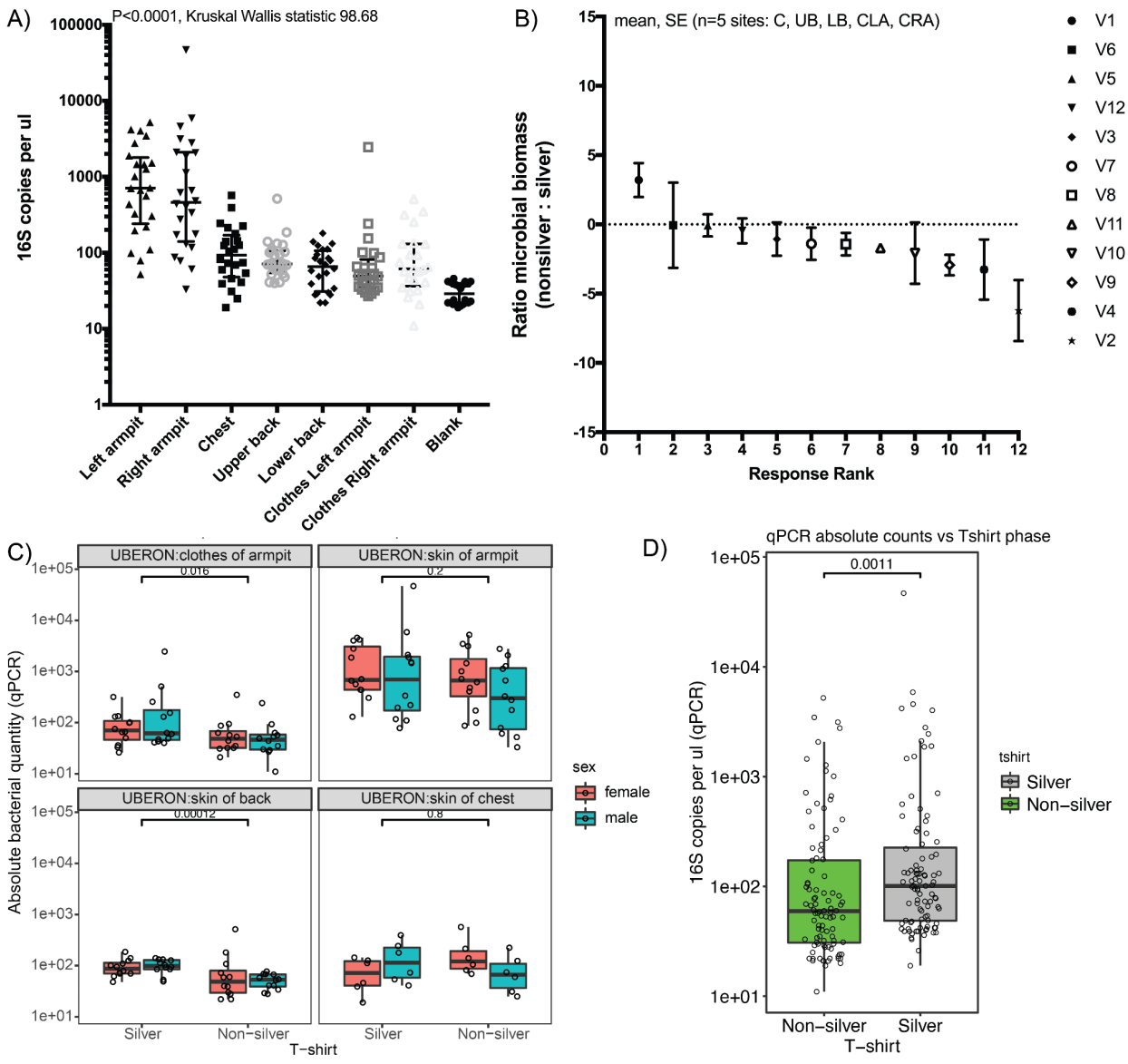

Supplementary Figure 5

Absolute 16S rRNA gene quantitation of week 8 and week 11 by body site and t-shirt type (non-silver or silver). a) The 16S rRNA gene copies per ul is calculated per the 12 participants with silver and non-silver t-shirts and grouped by body site location. Non-parametric Kruskal Wallis test (P<0.0001, Kruskal-Wallis test 98.68) demonstrates that 16S rRNA gene copy number varies per body site. Multiple comparisons testing and Benjamini & Hochberg FDR correction indicates that the left and right armpit had higher bacterial counts than all other samples and did not differ from each other. b) Bacterial load in all samples separated by sampled volunteers and displayed as a ratio of non-silver to silver. All samples falling below the dotted line indicate the increase of the bacterial load during the silver phase. c) qPCR results represented for all samples separated by gender and body part and based on the t-shirt phase (silver vs. non-silver). d) qPCR results represented for all samples combined and separated based on the t-shirt phase (silver vs. non-silver).

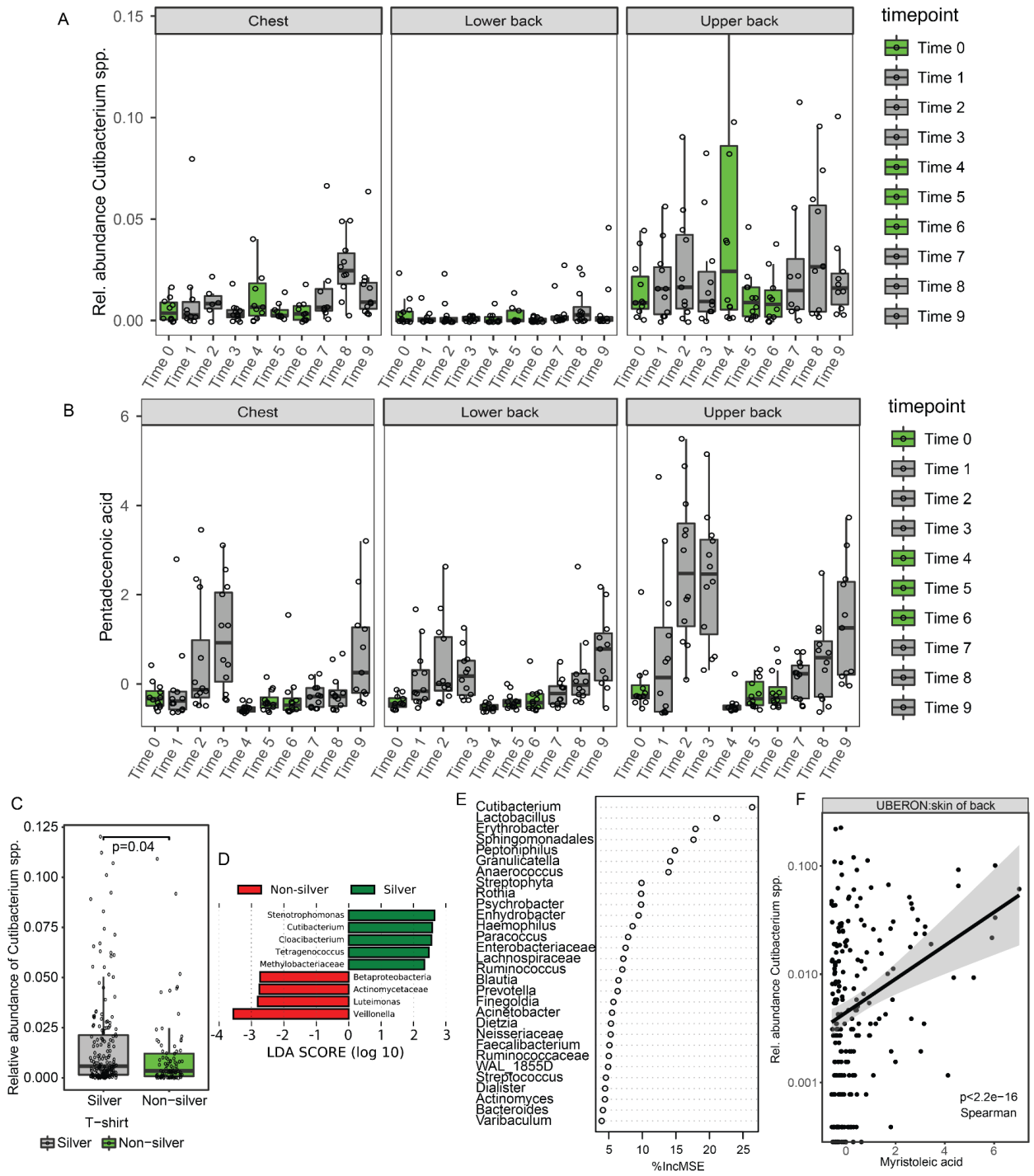

Supplementary Figure 6

Monounsaturated fatty acids and *Cutibacterium* spp. enriched in a silver phase. a) The relative abundance of *Cutibacterium* spp. increases during the silver t-shirt phase. b) The relative abundance of pentadecenoic acid (C15 fatty acid) increases during the silver t-shirt phase, while its abundance decreases during non-silver t-shirt phase, on both chest, lower back and upper back skin. c) The relative abundance of *Cutibacterium* spp. is higher on skin when silver shirts are worn. d) Cutibacterium spp. are enriched on shirts containing silver. e) Random Forest Regression analysis on bacterial taxa that are the

most affected by presence of Myristoleic acid. f) Significant Spearman correlation ($p<2.2e-16$) of myristoleic acid and the relativa abundance of *Cutibacterium* spp.

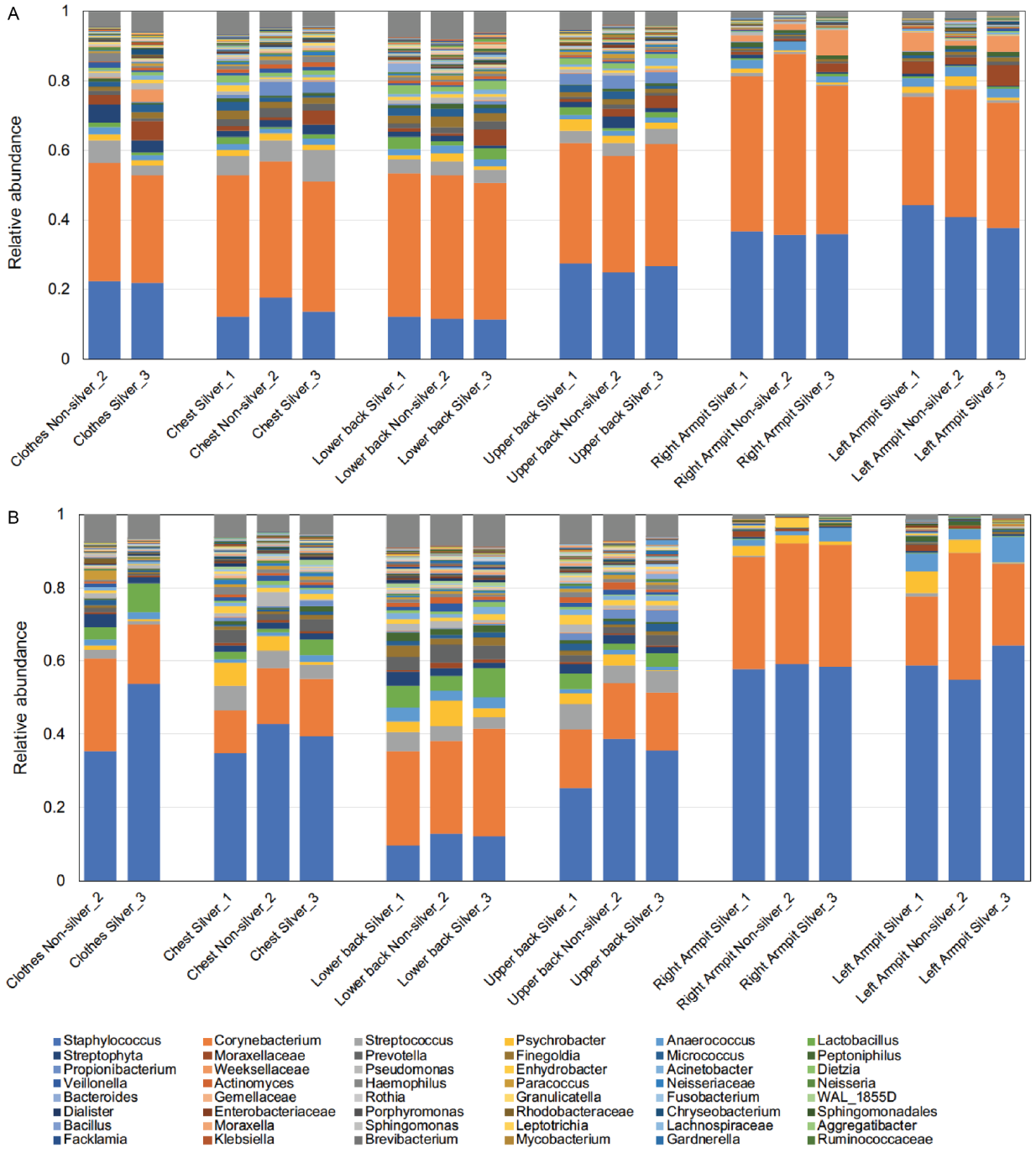

Supplementary Figure 7

Microbiome composition on clothes, chest, lower & upper back, right & left armpit for male a) and female b) participants. A total of 6 males and 6 females participated in the study. The major bacterial groups were not largely affected by silver, non-silver or back to silver shirt phase.

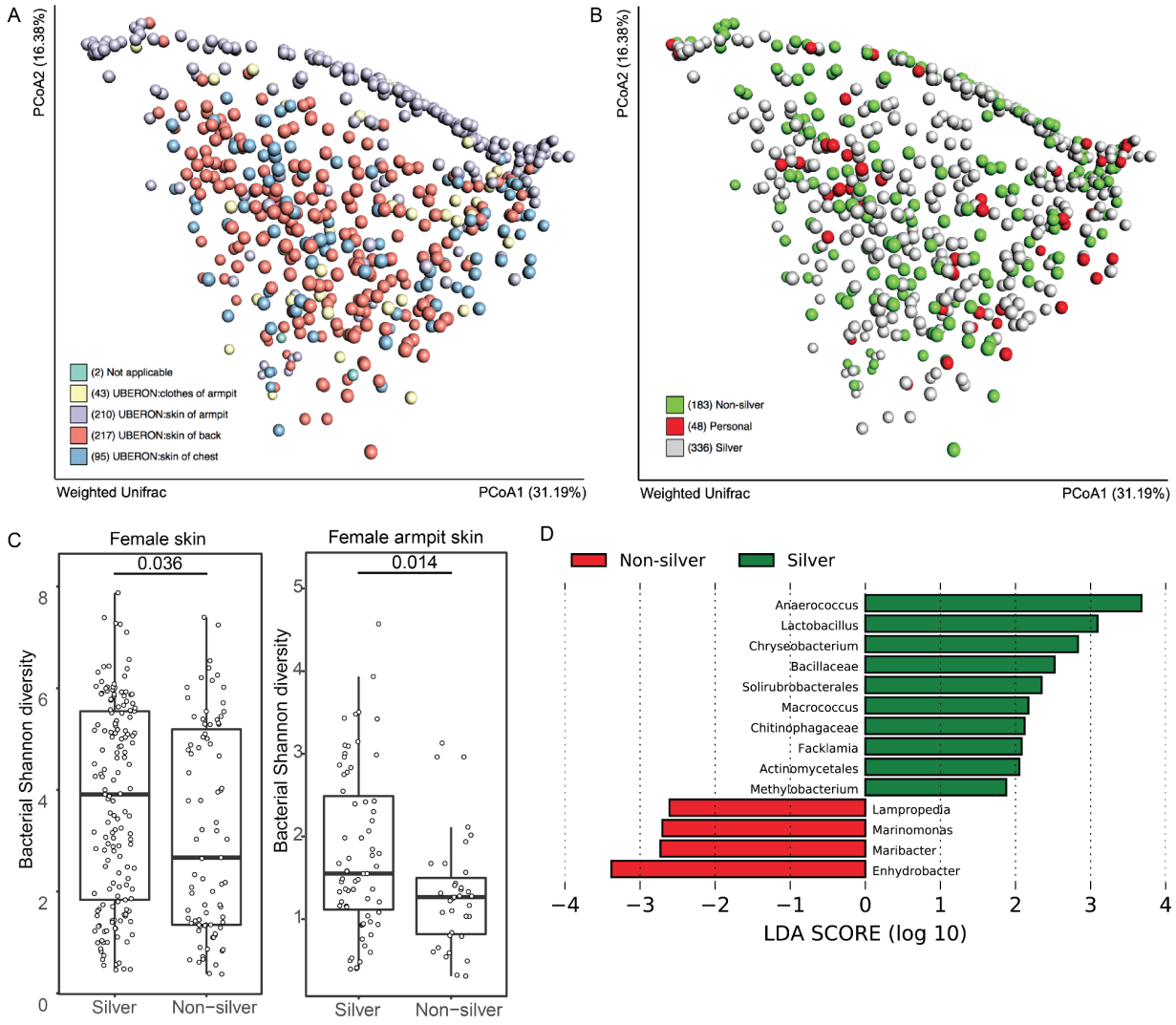

Supplementary Figure 8

a) Principal coordinate analysis showing clustering of microbiomes by body site (Adonis R^2=0.15738, p<0.001). b) Principal coordinate analysis showing little clustering of microbiomes by t-shirt (Adonis R^2=0.00601, p=0.017). c) Bacterial alpha diversity of the female skin and armpit microbiome. Significantly higher bacterial diversity is observed during the Silver phase. D) Underarm skin bacteriome enrichment of taxa on silver versus non-silver threaded shirt.

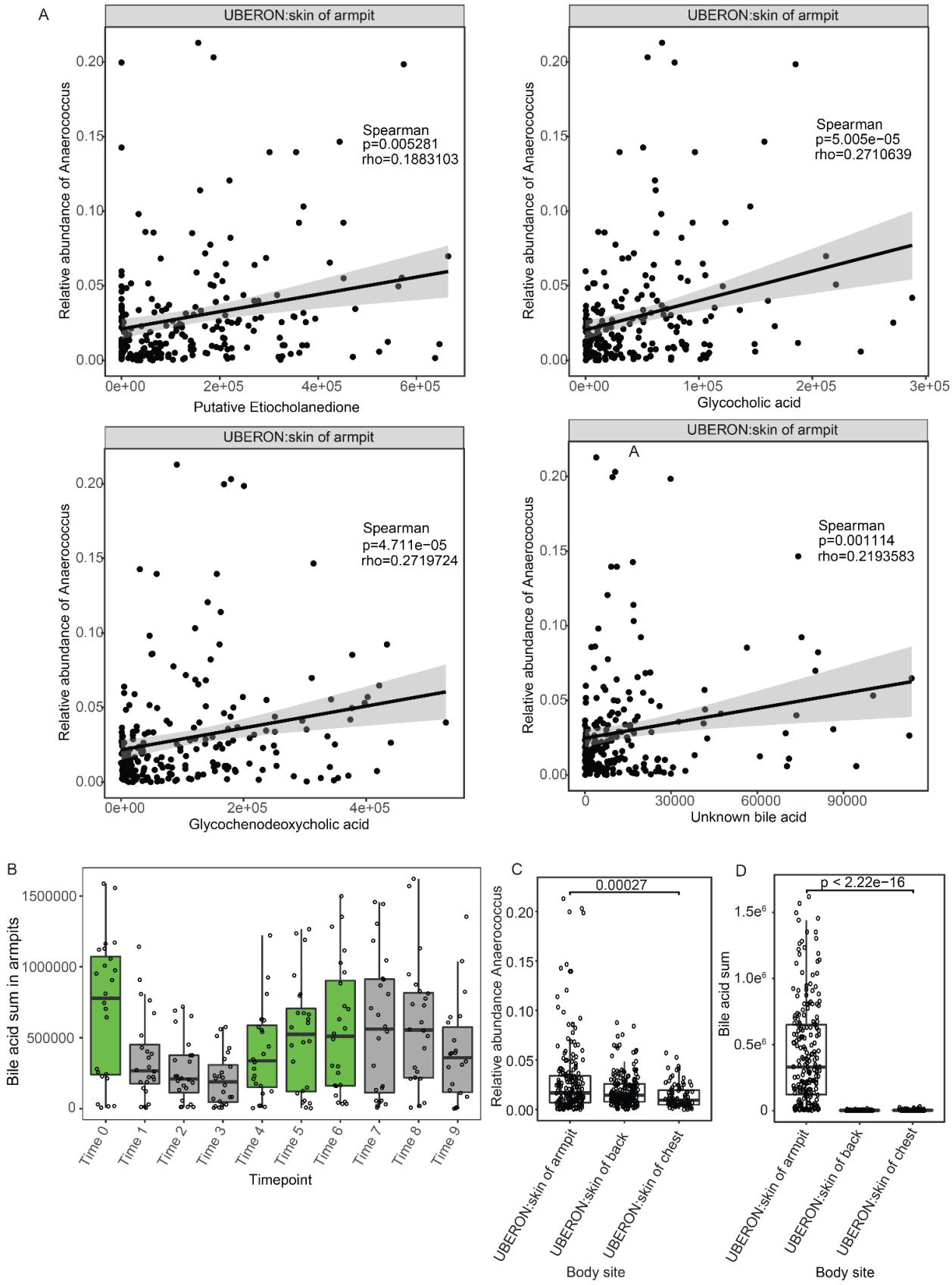
A
UBERON:skin of armpit
Relative abundance of Anaerococcus
Spearman
p=0.005281
rho=0.1883103
Putative Etiocholanedione
UBERON:skin of armpit
Spearman
p=5.005e−05
rho=0.2710639
Glycocholic acid
UBERON:skin of armpit
Spearman
p=4.711e−05
rho=0.2719724
Glycochenodeoxycholic acid
UBERON:skin of armpit
A
Spearman
p=0.001114
rho=0.2193583
Unknown bile acid
B
Bile acid sum in armpits
Time 0
Time 1
Time 2
Time 3
Time 4
Time 5
Time 6
Time 7
Time 8
Time 9
Timepoint
C
0.00027
Relative abundance Anaerococcus
UBERON:skin of armpit
UBERON:skin of back
UBERON:skin of chest
Body site
D
p < 2.22e−16
Bile acid sum
UBERON:skin of armpit
UBERON:skin of back
UBERON:skin of chest
Body site

Supplementary Figure 9

a) Spearman correlation of 4 major bile acids with *Anaerococcus* spp. b) Distribution of 4 bile acids across all timepoints for all volunteers combined and coloured by t-shirt phase, where green is non-silver phase and grey is silver phase. c) *Anaerococcus* spp. abundance plotted for armpits, back and chest d) Sum abundance of all 4 major bile acids plotted for armpits, back and chest, and armpits.

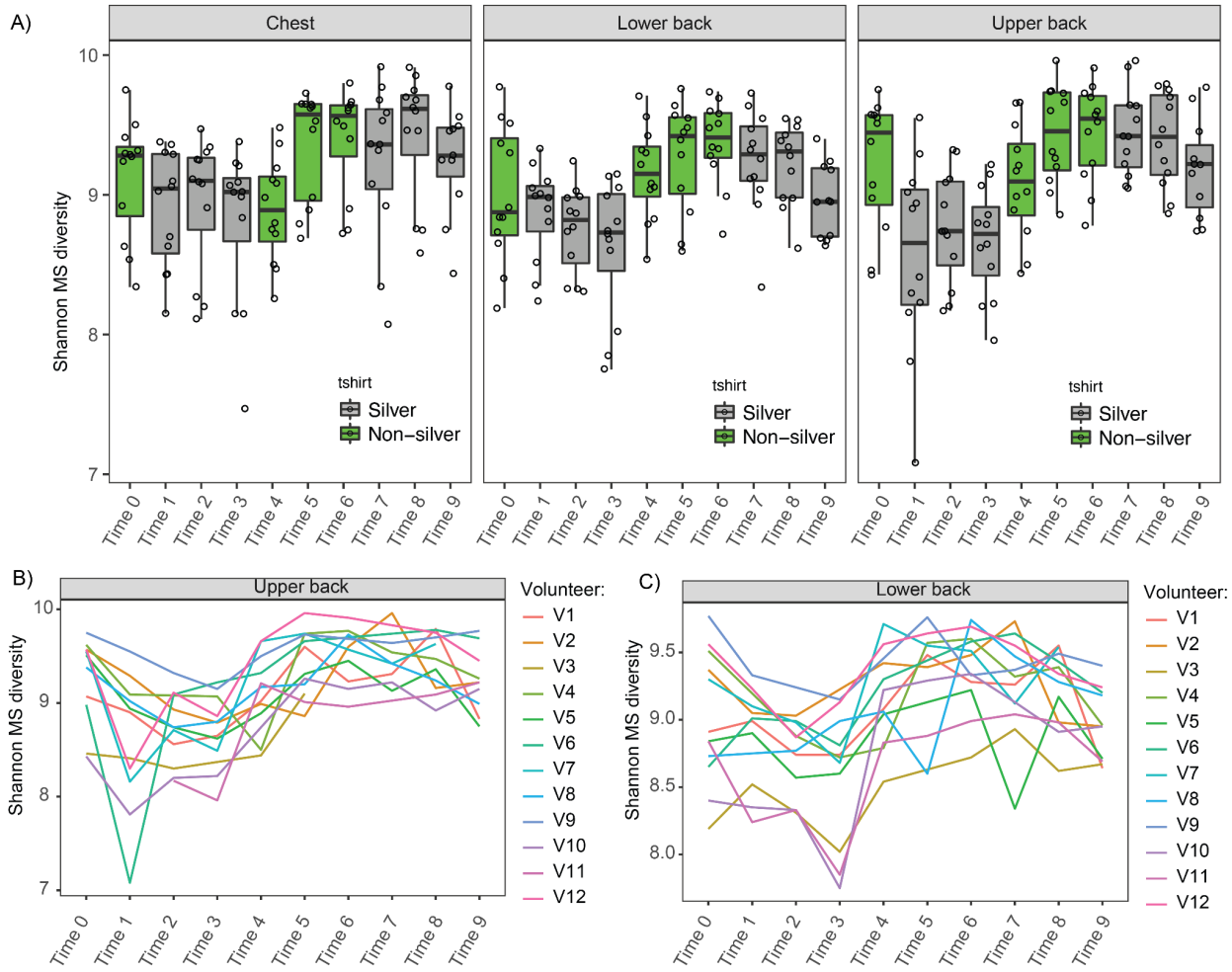

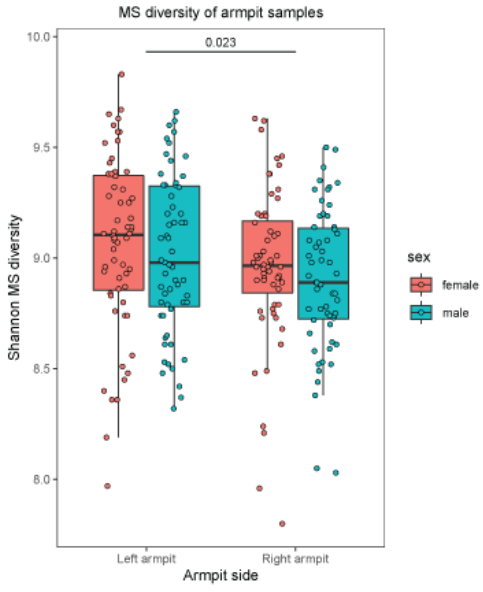

d)

Supplementary Figure 10

Shannon chemical (MS) diversity over time for chest, lower back and upper back. Metabolic Shannon decreases during the silver phase and increases during the non-silver phase. The impact is clearly seen on the skin sites with the most interaction with the textiles. Also in an individual manner the effect is clearly seen (panel B and C). d) Chemical diversity for all volunteers' armpit samples separated by side and coloured by the gender.

T**able S1_Mzmine feature finding parameters**	**Feature findings for all features**
Mass detection	
Noise level	1000
Chromatogram builder	
Minimum time span	0.01 min
Minimum peak height	3000
m/z tolerance	0.1 m/z or 20 ppm
Chromatogram deconvolution	
Baseline cutoff	
Minimum peak height	3000
Peak duration range (min)	0.01 - 3.00
Baseline level	300
Deisotopisation	
Isotopic peak grouper	
m/z tolerance	0.1 m/z or 20 ppm
RT tolerance	0.1 min
Maximum charge	4
Peak alignment	
Join aligner	
m/z tolerance	0.1 m/z or 20 ppm
Weight for m/z	75
Weight for RT	25
RT tolerance (min)	0.1 min
Peak filtering	
Peak list raw filter	
Minimum peak in a row	3
Minimum peak in an isotope pattern	2

Supplementary Table 1.

MzMine[53] feature detection parameters.[59]

References

1. Dąbrowska, J., Wójcik, M., Boreński, G. & Bator, D. Influence of diet on the gut microbiota. *Journal of Education* (2020).
2. Van Herreweghen, F., Amberg, C., Marques, R. & Callewaert, C. Biological and Chemical Processes that Lead to Textile Malodour Development. *Microorganisms* vol. 8 1709 (2020).
3. Moissl-Eichinger, C., Berg, G. & Grube, M. *Microbiome Interplay and Control*. (Frontiers Media SA, 2018).
4. Jablonski, N. G. *Skin: A Natural History*. (University of California Press, 2008).
5. Schommer, N. N. & Gallo, R. L. Structure and function of the human skin microbiome. *Trends Microbiol.* **21**, 660–668 (2013).
6. Byrd, A. L., Belkaid, Y. & Segre, J. A. The human skin microbiome. *Nat. Rev. Microbiol.* **16**, 143–155 (2018).
7. Naik, S. *et al.* Compartmentalized control of skin immunity by resident commensals. *Science* **337**, 1115–1119 (2012).
8. Scharschmidt, T. C. & Fischbach, M. A. What Lives On Our Skin: Ecology, Genomics and Therapeutic Opportunities Of the Skin Microbiome. *Drug Discov. Today Dis. Mech.* **10**, (2013).
9. Broadhead, R., Craeye, L. & Callewaert, C. The Future of Functional Clothing for an Improved Skin and Textile Microbiome Relationship. *Microorganisms* **9**, (2021).
10. Elpa, D. P., Chiu, H.-Y., Wu, S.-P. & Urban, P. L. Skin Metabolomics. *Trends Endocrinol. Metab.* **32**, 66–75 (2021).
11. Jacques, C. *et al.* Effect of skin metabolism on dermal delivery of testosterone: qualitative assessment using a new short-term skin model. *Skin Pharmacol. Physiol.* **27**, 188 (2014).
12. Zuber, R., Anzenbacherová, E. & Anzenbacher, P. Cytochromes P450 and experimental

models of drug metabolism. *J. Cell. Mol. Med.* **6**, 189–198 (2002).

13. Paliwal, S., Hwang, B. H., Tsai, K. Y. & Mitragotri, S. Diagnostic opportunities based on skin biomarkers. *Eur. J. Pharm. Sci.* **50**, 546–556 (2013).
14. Ji, Y., Guo, S. & Yang, Y. Research progress of metabolomics strategies. *J Anhui Agri Sci* **25**, 21–23 (2015).
15. McCall, L.-I. *et al.* Home chemical and microbial transitions across urbanization. *Nature Microbiology* vol. 5 108–115 (2020).
16. Hoefer, D. & Hammer, T. R. Antimicrobial active clothes display no adverse effects on the ecological balance of the healthy human skin microflora. *ISRN Dermatol.* **2011**, 369603 (2011).
17. Avagyan, R., Luongo, G., Thorsén, G. & Östman, C. Benzothiazole, benzotriazole, and their derivates in clothing textiles—a potential source of environmental pollutants and human exposure. *Environ. Sci. Pollut. Res.* **22**, 5842–5849 (2014).
18. Grass, G., Rensing, C. & Solioz, M. Metallic Copper as an Antimicrobial Surface. *Appl. Environ. Microbiol.* **77**, 1541–1547 (2010).
19. Gotzmann, G., Fraunhofer Institute for Organic Electronics & Electron Beam and Plasma Technology FEP. Silver/Copper-mixed Layers as Antimicrobial Surface Coating. in *60th Annual Technical Conference Proceedings* (2018). doi:10.14332/svc17.proc.42887.
20. McQueen, R. H., Laing, R. M., Delahunty∗, C. M., Brooks, H. J. L. & Niven, B. E. Retention of axillary odour on apparel fabrics. *Journal of the Textile Institute* vol. 99 515–523 (2008).
21. Troccaz, M. *et al.* Mapping axillary microbiota responsible for body odours using a culture-independent approach. *Microbiome* **3**, 3 (2015).
22. Wang, M. *et al.* Sharing and community curation of mass spectrometry data with Global Natural Products Social Molecular Networking. *Nat. Biotechnol.* **34**, 828–837 (2016).

23. Bouslimani, A. *et al.* The impact of skin care products on skin chemistry and microbiome dynamics. *BMC Biol.* **17**, 47 (2019).
24. Vázquez-Baeza, Y., Pirrung, M., Gonzalez, A. & Knight, R. EMPeror: a tool for visualizing high-throughput microbial community data. *Gigascience* **2**, 16 (2013).
25. Callewaert, C. *et al.* Characterization of Staphylococcus and Corynebacterium clusters in the human axillary region. *PLoS One* **8**, e70538 (2013).
26. Sim, W., Barnard, R., Blaskovich, M. A. T. & Ziora, Z. Antimicrobial Silver in Medicinal and Consumer Applications: A Patent Review of the Past Decade (2007–2017). *Antibiotics* vol. 7 93 (2018).
27. Morton, J. T. *et al.* Learning representations of microbe-metabolite interactions. *Nat. Methods* **16**, 1306–1314 (2019).
28. Haase, H., Jordan, L., Keitel, L., Keil, C. & Mahltig, B. Comparison of methods for determining the effectiveness of antibacterial functionalized textiles. *PLoS One* **12**, e0188304 (2017).
29. Sterndorff, E. B. *et al.* The T-shirt microbiome is distinct between individuals and shaped by washing and fabric type. *Environ. Res.* **185**, 109449 (2020).
30. Maillard, J.-Y. & Hartemann, P. Silver as an antimicrobial: facts and gaps in knowledge. *Crit. Rev. Microbiol.* **39**, 373–383 (2013).
31. Wu, H. & San, K.-Y. Efficient odd straight medium chain free fatty acid production by metabolically engineered Escherichia coli. *Biotechnol. Bioeng.* **111**, 2209–2219 (2014).
32. Jenkins, B., West, J. A. & Koulman, A. A review of odd-chain fatty acid metabolism and the role of pentadecanoic Acid (c15:0) and heptadecanoic Acid (c17:0) in health and disease. *Molecules* **20**, 2425–2444 (2015).
33. Zhang, L.-S., Liang, S., Zong, M.-H., Yang, J.-G. & Lou, W.-Y. Microbial synthesis of

functional odd-chain fatty acids: a review. *World J. Microbiol. Biotechnol.* **36**, 35 (2020).

34. Nikkari, T. Comparative Chemistry of Sebum. *Journal of Investigative Dermatology* vol. 62 257–267 (1974).
35. Nicolaides, N., Kellum, R. E. & Woolley, P. V., 3rd. THE STRUCTURES OF THE FREE UNSATURATED FATTY ACIDS OF HUMAN SKIN SURFACE FAT. *Arch. Biochem. Biophys.* **105**, 634–639 (1964).
36. Barzantny, H. *et al.* The transcriptional regulatory network of Corynebacterium jeikeium K411 and its interaction with metabolic routes contributing to human body odor formation. *J. Biotechnol.* **159**, 235–248 (2012).
37. Barzantny, H., Brune, I. & Tauch, A. Molecular basis of human body odour formation: insights deduced from corynebacterial genome sequences. *Int. J. Cosmet. Sci.* **34**, 2–11 (2012).
38. Hiltunen, J. K., Kalervo Hiltunen, J. & Qin, Y.-M. β-Oxidation – strategies for the metabolism of a wide variety of acyl-CoA esters. *Biochimica et Biophysica Acta (BBA) - Molecular and Cell Biology of Lipids* vol. 1484 117–128 (2000).
39. Brüggemann, H. Skin: Cutibacterium (formerly Propionibacterium) acnes and Acne Vulgaris. *Health Consequences of Microbial Interactions with Hydrocarbons, Oils, and Lipids* 225–243 (2020) doi:10.1007/978-3-030-15147-8_20.
40. Roux, P.-F., Oddos, T. & Stamatas, G. Deciphering the Role of Skin Surface Microbiome in Skin Health: An Integrative Multiomics Approach Reveals Three Distinct Metabolite–Microbe Clusters. *J. Invest. Dermatol.* (2021) doi:10.1016/j.jid.2021.07.159.
41. Chen, Z.-S., Guo, Y., Belinsky, M. G., Kotova, E. & Kruh, G. D. Transport of Bile Acids, Sulfated Steroids, Estradiol 17-β-d-Glucuronide, and Leukotriene C4 by Human Multidrug Resistance Protein 8 (ABCC11). *Molecular Pharmacology* vol. 67 545–557 (2005).

42. Bouslimani, A. *et al.* Molecular cartography of the human skin surface in 3D. *Proc. Natl. Acad. Sci. U. S. A.* **112**, E2120–9 (2015).
43. Jia, L. *et al.* NPC1L1 Deficiency Suppresses Ileal Fibroblast Growth Factor 15 Expression and Increases Bile Acid Pool Size in High-Fat-Diet-Fed Mice. *Cells* **10**, (2021).
44. Inagaki, T. *et al.* Regulation of antibacterial defense in the small intestine by the nuclear bile acid receptor. *Proc. Natl. Acad. Sci. U. S. A.* **103**, 3920–3925 (2006).
45. Tian, Y. *et al.* The microbiome modulating activity of bile acids. *Gut Microbes* **11**, 979–996 (2020).
46. Ruiz, L., Margolles, A. & Sánchez, B. Bile resistance mechanisms in Lactobacillus and Bifidobacterium. *Front. Microbiol.* **4**, 396 (2013).
47. Thompson, L. R. *et al.* A communal catalogue reveals Earth's multiscale microbial diversity. *Nature* vol. 551 457–463 (2017).
48. Walters, W. *et al.* Improved Bacterial 16S rRNA Gene (V4 and V4-5) and Fungal Internal Transcribed Spacer Marker Gene Primers for Microbial Community Surveys. *mSystems* **1**, (2016).
49. Caporaso, J. G. *et al.* QIIME allows analysis of high-throughput community sequencing data. *Nat. Methods* **7**, 335–336 (2010).
50. Edgar, R. C. Search and clustering orders of magnitude faster than BLAST. *Bioinformatics* **26**, 2460–2461 (2010).
51. McDonald, D. *et al.* An improved Greengenes taxonomy with explicit ranks for ecological and evolutionary analyses of bacteria and archaea. *ISME J.* **6**, 610–618 (2012).
52. Protsyuk, I. *et al.* 3D molecular cartography using LC–MS facilitated by Optimus and 'ili software. *Nat. Protoc.* **13**, 134–154 (2017).
53. Pluskal, T., Castillo, S., Villar-Briones, A. & Orešič, M. MZmine 2: Modular framework for

processing, visualizing, and analyzing mass spectrometry-based molecular profile data. *BMC Bioinformatics* **11**, 1–11 (2010).

54. Morton, J. T. *et al.* Establishing microbial composition measurement standards with reference frames. *Nat. Commun.* **10**, 2719 (2019).
55. Fedarko, M. W. *et al.* Visualizing ’omic feature rankings and log-ratios using Qurro. *NAR Genomics and Bioinformatics* vol. 2 (2020).
56. Verikas, A., Gelzinis, A. & Bacauskiene, M. Mining data with random forests: A survey and results of new tests. *Pattern Recognit.* **44**, 330–349 (2011).
57. Segata, N. *et al.* Metagenomic biomarker discovery and explanation. *Genome Biol.* **12**, R60 (2011).
58. Ernst, M. *et al.* MolNetEnhancer: Enhanced Molecular Networks by Integrating Metabolome Mining and Annotation Tools. *Metabolites* **9**, 144 (2019).
59. Melnik, A. V. *et al.* Coupling Targeted and Untargeted Mass Spectrometry for Metabolome-Microbiome-Wide Association Studies of Human Fecal Samples. *Anal. Chem.* **89**, 7549–7559 (2017).